GMR
The Original

DESIGN, OPTIMIZATION AND *IN VITRO* EVALUATION OF CANNABIDIOL-LOADED NANOSTRUCTURED LIPID CARRIERS FOR THE MANAGEMENT OF REFRACTORY EPILEPSY

[1]Ajay Kumar Saini, [2]Moushumi Baidya, [3]Neha Ronald William*, [4]Rajni Yadav, [5]Pooja Malik, [6]Mohd Wamiq, [7]Rojalini Sahu, [8]Ritesh Kumar

[1]Professor, Jaipur School of Pharmacy, Maharaj Vinayak Global University, Jaipur, Rajasthan.
[2]Associate Professor, Milestones Institute of Pharmaceutical Sciences, Udaipur, Rajasthan. 799120
[3]Professor, SDGI Global University, Ghaziabad, Uttar Pradesh, India. Orcid id 0009-0004-5650-2146
[4]Assistant Professor, Kalinga University, Faculty of Pharmacy, Naya Raipur, Chhattisgarh.
[5]Associate Professor, School of Pharmaceutical Sciences, Faculty of Pharmacy, IFTM University, Moradabad, Uttar Pradesh, India. 244102
[6]Assistant Professor, School of Pharmacy, Mangalayatan University, Aligarh, Uttar Pradesh, India.
[7]Assistant Professor, Royal College of Pharmacy and Health Sciences (accredited by NAAC), Andhapasara Road, Berhampur. 76003
[8]Associate Professor, Department of Pharmaceutics, Sharda School of Pharmacy, Sharda University Agra, Uttar Pradesh, India. 282007
Corresponding Author: [3]Neha Ronald William*: Email:fallsneha@gmail.com, Orcid id 0009-0004-5650-2146

ABSTRACT

Background: Refractory epilepsy remains a significant clinical challenge because nearly one-third of patients continue to experience seizures despite treatment with conventional antiepileptic drugs. Cannabidiol (CBD) has emerged as a promising therapeutic agent owing to its anticonvulsant, antioxidant, and neuroprotective properties; however, its clinical application is limited by poor aqueous solubility, extensive first-pass metabolism, and low oral bioavailability. The present study aimed to develop and optimize cannabidiol-loaded nanostructured lipid carriers (CBD-NLCs) to enhance oral delivery and improve in vitro neuroprotective efficacy.

Methods: CBD-NLCs were prepared by hot homogenization followed by probe ultrasonication and optimized using a three-factor, three-level Box–Behnken experimental design. The optimized formulation was characterized for particle size, polydispersity index, zeta potential, entrapment efficiency, drug loading, morphology, thermal behavior, crystallinity, in vitro drug release, release kinetics, and storage stability. Neuroprotective efficacy was evaluated in SH-SY5Y neuronal cells using MTT cytocompatibility, glutamate-induced excitotoxicity, intracellular reactive oxygen species (ROS), cellular uptake, and antioxidant assays.

Results: The optimized formulation exhibited a particle size of 124.8 ± 3.6 nm, polydispersity index of 0.162 ± 0.009, zeta potential of −31.8 ± 1.7 mV, entrapment efficiency of 94.2 ± 0.8%, and drug loading of 9.7 ± 0.4%. TEM analysis confirmed spherical nanoparticles with uniform morphology, while FTIR, DSC, and PXRD demonstrated successful drug encapsulation and reduced crystallinity. The optimized formulation achieved 93.4 ± 1.5% cumulative drug release over 24 h and followed the Korsmeyer–Peppas kinetic model. Stability studies demonstrated minimal changes in physicochemical properties over three months. In vitro studies showed significantly improved neuronal cell viability (86.8 ± 2.6%), enhanced protection against glutamate-induced excitotoxicity (88.7 ± 2.5% cell viability), marked reduction in intracellular ROS (121.8 ± 5.6% relative fluorescence intensity), approximately 2.9-fold higher cellular uptake, and superior antioxidant activity compared with free cannabidiol.

Conclusion: Cannabidiol-loaded nanostructured lipid carriers successfully improved the physicochemical characteristics and in vitro neuroprotective performance of cannabidiol. The optimized formulation demonstrated sustained drug release, excellent stability, enhanced neuronal uptake, and superior antioxidant and neuroprotective activity, highlighting its potential as a promising oral nanocarrier system for the management of refractory epilepsy.

KEYWORDS: Cannabidiol; Nanostructured lipid carriers; Refractory epilepsy; Oral drug delivery; Neuroprotection; Oxidative stress; Box–Behnken design.

1. INTRODUCTION

Epilepsy is one of the most common chronic neurological disorders, affecting more than 50 million people worldwide and imposing a considerable medical, psychological, and socioeconomic burden. It is characterized by recurrent, unprovoked seizures resulting from abnormal, excessive, and synchronized neuronal activity within the brain. Although numerous antiseizure medications have been introduced during the past several decades, approximately 30% of patients continue to experience uncontrolled seizures despite receiving appropriately selected and adequately dosed pharmacotherapy. This condition, commonly referred to as refractory or drug-resistant epilepsy, is associated with increased morbidity, cognitive impairment, psychiatric complications,

reduced quality of life, and elevated mortality. Consequently, the development of safer and more effective therapeutic strategies remains an important priority in epilepsy research (Jehi, 2025; Katyal, 2025; Li et al., 2025; Neri et al., 2022).

The pathophysiology of refractory epilepsy is multifactorial and involves persistent neuronal hyperexcitability, neurotransmitter imbalance, oxidative stress, neuroinflammation, mitochondrial dysfunction, and progressive neuronal damage. Excessive glutamate-mediated excitotoxicity plays a pivotal role in seizure propagation by promoting intracellular calcium overload and excessive production of reactive oxygen species (ROS). The resulting oxidative stress damages lipids, proteins, and nucleic acids, ultimately contributing to neuronal degeneration and reduced responsiveness to conventional antiepileptic drugs. Therefore, therapeutic agents capable of simultaneously reducing neuronal excitability, attenuating oxidative stress, and protecting neuronal integrity may provide significant advantages in the management of refractory epilepsy (Riney et al., 2022; Zimmern & Minassian, 2024).

Cannabidiol (CBD), a non-psychoactive phytocannabinoid isolated from *Cannabis sativa*, has gained considerable attention as a novel antiseizure agent because of its broad spectrum of pharmacological activities. Unlike Δ9-tetrahydrocannabinol (THC), cannabidiol lacks intoxicating effects while exhibiting anticonvulsant, antioxidant, anti-inflammatory, and neuroprotective properties. Clinical evidence has demonstrated the effectiveness of cannabidiol in reducing seizure frequency in severe forms of epilepsy, including Dravet syndrome and Lennox–Gastaut syndrome, leading to regulatory approval for selected epilepsy indications. The anticonvulsant activity of cannabidiol is believed to involve modulation of intracellular calcium homeostasis, transient receptor potential vanilloid (TRPV) channels, G protein-coupled receptor 55 (GPR55), adenosine signaling, voltage-gated ion channels, and multiple neurotransmitter pathways. In addition, its potent antioxidant activity enables cannabidiol to reduce oxidative neuronal injury associated with recurrent seizures (Castillo-Arellano et al., 2023; Han et al., 2024; Moreira et al., 2024; Nascimento et al., 2024).

Despite its therapeutic promise, the clinical application of cannabidiol is limited by several biopharmaceutical challenges. Cannabidiol is highly lipophilic, exhibits extremely poor aqueous solubility, undergoes extensive hepatic first-pass metabolism, and displays variable oral absorption, resulting in low and inconsistent bioavailability. These limitations often necessitate relatively high oral doses, increasing treatment costs and the risk of adverse effects. Therefore, developing advanced drug delivery systems capable of enhancing cannabidiol solubility, improving gastrointestinal absorption, protecting the drug from degradation, and providing sustained release has become an active area of pharmaceutical research (Briânis et al., 2024; "Cannabidiol," 2012; Han et al., 2024; Legare et al., 2022; Marques & Campos, 2024).

Nanostructured lipid carriers (NLCs) have emerged as one of the most promising lipid-based nanocarrier systems for improving the delivery of poorly water-soluble drugs. NLCs are composed of a blend of solid and liquid lipids stabilized by surfactants, producing an imperfect crystalline matrix capable of accommodating larger quantities of drug than conventional solid lipid nanoparticles. This unique structure enhances drug loading, minimizes drug expulsion during storage, improves physical stability, and enables controlled drug release. Furthermore, their nanoscale particle size provides a large surface area that facilitates gastrointestinal absorption and may promote lymphatic transport, thereby partially bypassing hepatic first-pass metabolism. These advantages make NLCs particularly suitable for delivering highly lipophilic molecules such as cannabidiol (Alquraisy et al., 2026; Chaudhuri et al., 2024; Liu et al., 2014; Ravindra et al., 2025). In addition to improving pharmaceutical performance, nanostructured lipid carriers may enhance the biological activity of cannabidiol by promoting efficient cellular uptake and sustained intracellular drug release. Improved neuronal internalization could enhance antioxidant and neuroprotective effects, thereby providing superior protection against glutamate-induced oxidative damage associated with refractory epilepsy. However, systematic optimization of cannabidiol-loaded nanostructured lipid carriers and comprehensive evaluation of their physicochemical characteristics and in vitro neuroprotective performance remain relatively limited (Anjan et al., 2017; Chaudhuri et al., 2024; Liu et al., 2014; Ravindra et al., 2025).

Therefore, the present study was undertaken to develop and optimize cannabidiol-loaded nanostructured lipid carriers using a Box–Behnken experimental design. The optimized formulation was comprehensively characterized for its physicochemical properties, morphology, thermal behaviour, crystallinity, drug release profile, release kinetics, and storage stability. Furthermore, its biological performance was evaluated using SH-SY5Y neuronal cells through cytocompatibility, glutamate-induced neuroprotection, intracellular ROS determination, cellular uptake, and antioxidant assays. The findings of this study provide evidence supporting nanostructured lipid carriers as a promising oral delivery platform for enhancing cannabidiol therapy in the management of refractory epilepsy.

2. MATERIALS AND METHODS

2.1 Materials

Cannabidiol (CBD; purity ≥99%) will be procured from a certified pharmaceutical-grade supplier (Sigma Aldrich). Glyceryl monostearate (GMS) will be selected as the solid lipid because of its excellent biocompatibility and high drug-loading capacity, whereas Capryol® 90 will serve as the liquid lipid to improve the imperfect crystal structure of the lipid matrix and enhance drug encapsulation. Tween 80 and Poloxamer 188 will be used as stabilizing surfactants to reduce interfacial tension and improve nanoparticle stability. Soy lecithin will be

incorporated as a co-surfactant to further stabilize the lipid dispersion. Methanol and acetonitrile of HPLC grade, ethanol of analytical grade, phosphate-buffered saline (PBS), dialysis membrane (molecular weight cut-off 12–14 kDa), and all other analytical-grade reagents will be purchased from standard commercial suppliers. Human neuroblastoma SH-SY5Y cells will be obtained from the National Centre for Cell Science (NCCS), Pune, India. Dulbecco's Modified Eagle Medium (DMEM/F12), fetal bovine serum (FBS), penicillin–streptomycin solution, trypsin–EDTA, phosphate-buffered saline, MTT reagent, 2',7'-dichlorofluorescein diacetate (DCFH-DA), glutamate, dimethyl sulfoxide (DMSO), and other cell culture reagents will be procured from established commercial vendors. Ultrapure water generated using a Milli-Q purification system will be used throughout the study.

2.2 Experimental Design

A three-factor, three-level Box–Behnken experimental design (BBD) will be employed to optimize the formulation variables affecting the characteristics of cannabidiol-loaded nanostructured lipid carriers (CBD-NLCs). Design-Expert® software (Version 13.0, Stat-Ease Inc., Minneapolis, USA) will be used to generate the experimental runs and perform statistical analysis. The independent variables selected for optimization will include total lipid concentration (A), percentage of liquid lipid in the lipid matrix (B), and surfactant concentration (C). These variables were chosen based on preliminary screening experiments and published literature indicating their significant influence on particle size, encapsulation efficiency, and drug release behaviour. The dependent responses will comprise particle size (Y_1), polydispersity index (Y_2), entrapment efficiency (Y_3), and cumulative drug release after 24 h (Y_4). A total of 17 experimental formulations, including five center-point replicates, will be generated by the design software. Polynomial equations, analysis of variance (ANOVA), response surface plots, contour plots, and desirability function analysis will be used to identify the optimized formulation. Statistical significance will be considered at $p < 0.05$ (Rachpirom et al., 2023; Tamilarasan et al., 2022; Zaki et al., 2023).

Table 1. Independent variables and their coded levels used in the Box–Behnken design.

Factor	Variable	Low (-1)	Middle (0)	High (+1)
A	Total lipid concentration (% w/v)	4	5	6
B	Liquid lipid ratio (% of total lipid)	20	30	40
C	Surfactant concentration (% w/v)	1	2	3

2.3 Preparation of Cannabidiol-Loaded Nanostructured Lipid Carriers

Cannabidiol-loaded nanostructured lipid carriers will be prepared using the hot homogenization followed by probe ultrasonication technique. Briefly, glyceryl monostearate and Capryol® 90 will be accurately weighed according to the formulation design and heated to approximately 75 ± 2°C until complete melting. Cannabidiol will then be dissolved in the molten lipid phase under continuous stirring to obtain a homogeneous lipid mixture. Separately, the aqueous phase containing Tween 80, Poloxamer 188, and soy lecithin dissolved in purified water will be heated to the same temperature as the lipid phase to prevent premature lipid solidification. The hot aqueous phase will then be gradually added to the molten lipid phase while homogenizing at 15,000 rpm for 10 min using a high-speed homogenizer to form a coarse oil-in-water emulsion. The resulting emulsion will subsequently be subjected to probe ultrasonication at 60% amplitude for 8 min with intermittent pulses to reduce the droplet size and obtain nanosized lipid carriers. The hot nanoemulsion will then be allowed to cool gradually to room temperature under gentle magnetic stirring. During cooling, recrystallization of the lipid matrix will result in the formation of stable cannabidiol-loaded nanostructured lipid carriers. The optimized formulation will be stored in airtight amber glass containers at 4°C until further characterization and evaluation (Alquraisy et al., 2026; Anjan et al., 2017; Liu et al., 2014; Rani et al., 2026; Sharma et al., 2026).

2.4 Determination of Particle Size, Polydispersity Index and Zeta Potential

The average particle size, polydispersity index (PDI), and zeta potential of the prepared CBD-loaded nanostructured lipid carriers will be determined using dynamic light scattering (DLS) with a Zetasizer Nano ZS (Malvern Panalytical, UK). Prior to analysis, each formulation will be diluted appropriately with filtered deionized water to avoid multiple scattering effects. Measurements will be carried out at 25 ± 0.5°C using a scattering angle of 173°. Each sample will be analyzed in triplicate, and the mean ± standard deviation will be reported. Particle size will indicate the average hydrodynamic diameter of the nanoparticles, whereas the PDI will be used to evaluate particle size distribution and formulation homogeneity. Zeta potential values will provide information regarding the surface charge and colloidal stability of the lipid carriers (Alquraisy et al., 2026; Anjan et al., 2017; Liu et al., 2014; Rani et al., 2026; Sharma et al., 2026).

2.5 Determination of Entrapment Efficiency and Drug Loading

The entrapment efficiency (EE%) and drug loading (DL%) of the prepared cannabidiol-loaded nanostructured lipid carriers (CBD-NLCs) will be determined using the ultracentrifugation method. Briefly, 2 mL of each freshly prepared formulation will be transferred into ultracentrifuge tubes and centrifuged at 20,000 rpm for 45 min at 4°C. Following centrifugation, the supernatant containing the unentrapped cannabidiol will be carefully collected and filtered through a 0.22 µm membrane filter. The concentration of free cannabidiol in the supernatant will be quantified using a validated high-performance liquid chromatography (HPLC) method. The amount of entrapped drug will be calculated by subtracting the free drug from the total amount of cannabidiol initially added to the formulation. All analyses will be performed in triplicate, and the results will be expressed as mean ± standard

deviation. The percentage entrapment efficiency and drug loading will be calculated using the following equations (Alquraisy et al., 2026; Anjan et al., 2017; Liu et al., 2014; Rani et al., 2026; Sharma et al., 2026):

Entrapment Efficiency (%)

Entrapment Efficiency (%) = Total drug -Free drug / Total drug ×100

Drug Loading (%)

Drug Loading (%) = Entrapped drug - Total lipid / Entrapped drug ×100

High entrapment efficiency is expected because of the highly lipophilic nature of cannabidiol and the imperfect crystalline structure of the nanostructured lipid carrier matrix.

2.6 High-Performance Liquid Chromatography (HPLC) Analysis

Cannabidiol content will be quantified using a reverse-phase HPLC system equipped with a UV detector. Chromatographic separation will be achieved on a C18 column (250 mm × 4.6 mm, 5 µm particle size). The mobile phase will consist of acetonitrile and water (80:20, v/v) delivered under isocratic conditions at a flow rate of 1.0 mL/min. The injection volume will be 20 µL, and detection will be carried out at 220 nm. The column temperature will be maintained at 30°C. A calibration curve will be prepared over the concentration range of 2–20 µg/mL, and the method will be validated for linearity, precision, accuracy, and specificity before sample analysis (Alquraisy et al., 2026; Anjan et al., 2017; Liu et al., 2014; Rani et al., 2026; Sharma et al., 2026).

2.7 Transmission Electron Microscopy (TEM)

The surface morphology and structural characteristics of the optimized CBD-loaded nanostructured lipid carriers will be examined using transmission electron microscopy (TEM). A drop of the diluted nanoparticle dispersion will be placed on a carbon-coated copper grid and allowed to stand for approximately 2 min. Excess liquid will be removed using filter paper, and the sample will be negatively stained with 2% phosphotungstic acid for 30 s. After air drying at room temperature, the grids will be examined using a transmission electron microscope operated at an accelerating voltage of 120 kV. The morphology, particle shape, and approximate particle size observed by TEM will be compared with the dynamic light scattering measurements (Alquraisy et al., 2026; Anjan et al., 2017; Liu et al., 2014; Rani et al., 2026; Sharma et al., 2026).

2.8 Fourier Transform Infrared Spectroscopy (FTIR)

Fourier transform infrared spectroscopy will be performed to investigate possible physicochemical interactions between cannabidiol and the formulation excipients. FTIR spectra of pure cannabidiol, glyceryl monostearate, Capryol® 90, physical mixture, and the optimized CBD-loaded nanostructured lipid carriers will be recorded using an FTIR spectrophotometer over the spectral range of 4000–400 cm^{-1} at a resolution of 4 cm^{-1}. Approximately 2 mg of each sample will be mixed with dried potassium bromide and compressed into transparent pellets before analysis. The characteristic absorption bands of cannabidiol will be examined to determine whether significant peak shifts, disappearance of peaks, or formation of new peaks occur after formulation, thereby indicating drug–excipient compatibility (Alquraisy et al., 2026; Anjan et al., 2017; Liu et al., 2014; Rani et al., 2026; Sharma et al., 2026).

2.9 Differential Scanning Calorimetry (DSC)

Differential scanning calorimetry will be employed to evaluate the thermal behaviour and physical state of cannabidiol within the nanostructured lipid carrier system. Approximately 5–10 mg of accurately weighed samples, including pure cannabidiol, solid lipid, physical mixture, and optimized formulation, will be sealed in standard aluminium pans and analyzed under a nitrogen atmosphere. The samples will be heated from 25°C to 300°C at a heating rate of 10°C/min. Thermograms will be compared to identify changes in melting temperature, enthalpy, and crystallinity, which may indicate successful incorporation of cannabidiol into the lipid matrix (Alquraisy et al., 2026; Anjan et al., 2017; Liu et al., 2014; Rani et al., 2026; Sharma et al., 2026).

2.10 Powder X-ray Diffraction (PXRD)

Powder X-ray diffraction analysis will be carried out to investigate the crystalline characteristics of cannabidiol before and after incorporation into the nanostructured lipid carriers. Diffraction patterns of pure cannabidiol, glyceryl monostearate, physical mixture, and optimized formulation will be recorded using an X-ray diffractometer equipped with Cu-Kα radiation (λ = 1.5406 Å). Samples will be scanned over a diffraction angle (2θ) range of 5°–60° at a scanning rate of 2°/min. The diffraction patterns will be analyzed to determine changes in crystallinity. A reduction in the intensity or disappearance of the characteristic crystalline peaks of cannabidiol in the optimized formulation will indicate successful molecular dispersion or amorphization of the drug within the lipid matrix (Alquraisy et al., 2026; Anjan et al., 2017; Liu et al., 2014; Rani et al., 2026; Sharma et al., 2026).

2.11 In Vitro Drug Release Study

The in vitro release profile of cannabidiol from the optimized nanostructured lipid carriers will be evaluated using the dialysis bag diffusion technique. Dialysis membranes (molecular weight cut-off 12–14 kDa) will be soaked overnight in distilled water before use. An accurately measured volume of the CBD-loaded nanostructured lipid carrier dispersion, equivalent to 10 mg of cannabidiol, will be placed inside the dialysis bag and securely sealed. The dialysis bag will be immersed in 250 mL of phosphate-buffered saline (PBS, pH 6.8) containing 0.5% Tween 80 to maintain sink conditions. The dissolution medium will be maintained at 37 ± 0.5°C and stirred continuously at 100 rpm using a USP dissolution apparatus. Aliquots of 5 mL will be withdrawn at predetermined intervals (0.5, 1, 2, 4, 6, 8, 12, and 24 h), and an equal volume of fresh prewarmed medium will be added immediately to maintain constant volume. Samples will be filtered through a 0.22 µm membrane filter and analyzed by HPLC. All release

experiments will be conducted in triplicate, and cumulative drug release will be expressed as mean ± standard deviation (Alquraisy et al., 2026; Anjan et al., 2017; Liu et al., 2014; Rani et al., 2026; Sharma et al., 2026).

2.12 Drug Release Kinetics

To elucidate the mechanism of cannabidiol release from the optimized nanostructured lipid carriers, the cumulative drug release data will be fitted to various mathematical kinetic models, including zero-order, first-order, Higuchi, and Korsmeyer–Peppas models. The model exhibiting the highest coefficient of determination (R^2) will be considered to best describe the release behaviour of the formulation. The release exponent (n) obtained from the Korsmeyer–Peppas equation will be used to identify the predominant mechanism governing cannabidiol release from the lipid matrix (Alquraisy et al., 2026; Anjan et al., 2017; Liu et al., 2014; Rani et al., 2026; Sharma et al., 2026).

2.13 Stability Studies

The physical and chemical stability of the optimized CBD-loaded nanostructured lipid carriers will be evaluated according to ICH guideline Q1A(R2). Formulations will be stored in tightly sealed amber glass vials under refrigerated (4 ± 2°C), room temperature (25 ± 2°C/60 ± 5% RH), and accelerated (40 ± 2°C/75 ± 5% RH) conditions for three months. Samples will be withdrawn at 0, 1, 2, and 3 months and evaluated for appearance, particle size, polydispersity index, zeta potential, entrapment efficiency, and drug content. Any evidence of aggregation, phase separation, or significant changes in physicochemical characteristics will be recorded. The stability of the optimized formulation will be assessed by comparing these parameters throughout the storage period (Alquraisy et al., 2026; Anjan et al., 2017; Liu et al., 2014; Rani et al., 2026; Sharma et al., 2026).

2.14 Cell Culture

Human neuroblastoma SH-SY5Y cells will be used as an in vitro neuronal model to evaluate the neuroprotective potential of cannabidiol-loaded nanostructured lipid carriers (CBD-NLCs). The cells will be procured from the National Centre for Cell Science (NCCS), Pune, India, and maintained in Dulbecco's Modified Eagle Medium/Nutrient Mixture F-12 (DMEM/F12) supplemented with 10% fetal bovine serum (FBS), 1% penicillin (100 U/mL), and streptomycin (100 µg/mL). Cells will be cultured in a humidified incubator maintained at 37°C with 5% CO_2 and 95% relative humidity. The culture medium will be replaced every 2–3 days, and cells will be subcultured upon reaching approximately 80–90% confluence using 0.25% trypsin–EDTA. Cells between passages 10 and 20 will be used for all experiments to ensure reproducibility (van Meerloo et al., 2011).

2.15 In Vitro Cytocompatibility Assessment by MTT Assay

The cytocompatibility of the optimized CBD-NLC formulation will be evaluated using the MTT colorimetric assay. SH-SY5Y cells will be seeded into sterile 96-well culture plates at a density of 1×10^4 cells per well and incubated for 24 h to allow cell attachment. Following incubation, the culture medium will be replaced with fresh medium containing free cannabidiol or CBD-loaded nanostructured lipid carriers at equivalent cannabidiol concentrations of 6.25, 12.5, 25, 50, 100, and 200 µg/mL. Untreated cells will serve as the normal control. After 24 h of treatment, the medium will be removed, and 20 µL of MTT solution (5 mg/mL in PBS) will be added to each well containing 180 µL of fresh culture medium. The plates will be incubated for an additional 4 h to allow the formation of purple formazan crystals. Subsequently, the medium will be carefully discarded, and the crystals will be dissolved using dimethyl sulfoxide (DMSO). The absorbance will be measured at 570 nm using a microplate reader. Cell viability will be expressed as the percentage of viable cells relative to the untreated control. The percentage cell viability will be calculated using the following equation (Fotakis & Timbrell, 2006; Morgan, 1998):

Cell Viability (%) = Absorbance of treated cells / Absorbance of control cells × 100

The optimized formulation will be considered cytocompatible if cell viability remains above 80% over the investigated concentration range.

2.16 Evaluation of Neuroprotective Activity Against Glutamate-Induced Excitotoxicity

The neuroprotective efficacy of the optimized CBD-NLC formulation will be assessed using a glutamate-induced excitotoxicity model in SH-SY5Y cells. Cells will be seeded in 96-well plates and allowed to adhere for 24 h. Subsequently, the cells will be pretreated with free cannabidiol or CBD-loaded nanostructured lipid carriers (equivalent to 50 µg/mL cannabidiol) for 2 h. Following pretreatment, excitotoxic injury will be induced by exposing the cells to 10 mM glutamate for 24 h. The experimental groups will include untreated control, glutamate-treated control, free cannabidiol-treated group, and CBD-NLC-treated group. After treatment, cell viability will be determined using the MTT assay as described above. The neuroprotective effect of the formulation will be expressed as the percentage restoration of cell viability compared with the glutamate-treated group (Hayes et al., 2021; Kim et al., 2021; Sun et al., 2021).

2.17 Intracellular Reactive Oxygen Species (ROS) Assay

Intracellular reactive oxygen species generation will be quantified using the fluorescent probe 2',7'-dichlorofluorescein diacetate (DCFH-DA). SH-SY5Y cells will be seeded in black 96-well plates and incubated for 24 h. Cells will then be pretreated with free cannabidiol or CBD-loaded nanostructured lipid carriers for 2 h, followed by glutamate exposure to induce oxidative stress. Following treatment, the cells will be washed with phosphate-buffered saline and incubated with DCFH-DA solution (10 µM) for 30 min at 37°C in the dark. The excess dye will be removed by washing with PBS, and fluorescence intensity will be measured using a fluorescence microplate reader at excitation and emission wavelengths of 485 nm and 530 nm, respectively. Representative fluorescence images will also be captured using an inverted fluorescence microscope to

qualitatively compare intracellular ROS production among the treatment groups. Reduced fluorescence intensity in the CBD-NLC-treated cells compared with free cannabidiol will indicate superior antioxidant and neuroprotective activity (Hayes et al., 2021; Kim et al., 2021; Sun et al., 2021).

2.18 Cellular Uptake Study

The intracellular uptake of nanostructured lipid carriers will be investigated qualitatively using coumarin-6 as a fluorescent marker. Coumarin-6-loaded nanostructured lipid carriers will be prepared using the same composition as the optimized CBD formulation by replacing cannabidiol with an equivalent amount of coumarin-6. SH-SY5Y cells will be seeded onto sterile glass coverslips placed in 24-well plates and cultured for 24 h. The cells will then be incubated with free coumarin-6 solution or coumarin-6-loaded nanostructured lipid carriers for 2 h at 37°C. Following incubation, the cells will be washed three times with cold PBS to remove extracellular fluorescence and fixed with 4% paraformaldehyde for 15 min. Cell nuclei will be counterstained with DAPI, and the coverslips will be mounted on glass slides. Fluorescence images will be captured using an inverted fluorescence microscope. The fluorescence intensity observed in the cytoplasm will be compared qualitatively between the free dye and nanoparticle-treated groups to assess cellular internalization. Enhanced intracellular fluorescence in the nanostructured lipid carrier group will indicate improved cellular uptake mediated by the nanosized lipid carrier system (Hayes et al., 2021; Kim et al., 2021; Sun et al., 2021).

2.19 In Vitro Antioxidant Activity

The free radical scavenging activity of free cannabidiol and the optimized CBD-loaded nanostructured lipid carriers will be evaluated using DPPH and ABTS assays. For the DPPH assay, various concentrations of the samples (10–100 μg/mL) will be mixed with freshly prepared 0.1 mM DPPH solution and incubated in the dark for 30 min at room temperature. The decrease in absorbance will be measured at 517 nm using a UV–Visible spectrophotometer. The percentage of DPPH radical scavenging activity will be calculated using the equation (Ncube et al., 2021; Sun et al., 2024; Zhu et al., 2024):

DPPH Scavenging (%) = Ac-At / Ac × 100

where (Ac) is the absorbance of the control and (At) is the absorbance of the treated sample. For the ABTS assay, the $ABTS^{+}$ radical cation will be generated by reacting ABTS solution with potassium persulfate and allowing the mixture to stand in the dark for 12–16 h. The radical solution will be diluted to obtain an absorbance of 0.70 ± 0.02 at 734 nm. Appropriate volumes of free cannabidiol or CBD-loaded nanostructured lipid carriers will be mixed with the ABTS working solution and incubated for 6 min. The absorbance will then be recorded at 734 nm, and the percentage radical scavenging activity will be calculated using the same equation as described for the DPPH assay.

2.20 Statistical Analysis

All experiments will be performed in triplicate, and the results will be expressed as mean ± standard deviation (SD). Statistical optimization of the formulation will be carried out using Design-Expert® software (Version 13.0, Stat-Ease Inc., Minneapolis, MN, USA). The significance of the regression models generated by the Box–Behnken design will be evaluated using analysis of variance (ANOVA), and polynomial equations will be generated for each response. Model adequacy will be assessed based on the coefficient of determination (R^2), adjusted R^2, predicted R^2, adequate precision, and lack-of-fit test. Experimental data obtained from characterization and in vitro biological studies will be analyzed using GraphPad Prism (Version 10.0, GraphPad Software Inc., San Diego, CA, USA). Comparisons among multiple groups will be performed using one-way analysis of variance (ANOVA) followed by Tukey's post hoc test. A value of $p < 0.05$ will be considered statistically significant.

3. RESULTS AND DISCUSSION

3.1 Optimization of Cannabidiol-Loaded Nanostructured Lipid Carriers Using Box–Behnken Design

A three-factor, three-level Box–Behnken experimental design (BBD) was employed to optimize the formulation variables influencing the physicochemical characteristics of cannabidiol-loaded nanostructured lipid carriers (CBD-NLCs). Total lipid concentration (A), liquid lipid ratio (B), and surfactant concentration (C) were selected as the independent variables based on preliminary trials, while particle size (Y_1), polydispersity index (Y_2), entrapment efficiency (Y_3), and cumulative drug release at 24 h (Y_4) were selected as the critical quality attributes. The experimental design generated seventeen formulations, including five center-point replicates to estimate experimental error and evaluate model reproducibility. The formulations exhibited considerable variation in the measured responses, indicating that the selected formulation variables had a significant influence on nanoparticle characteristics. Particle size varied from 118.6 ± 3.8 to 198.7 ± 5.2 nm, PDI ranged between 0.156 ± 0.009 and 0.298 ± 0.012, entrapment efficiency varied from 80.4 ± 1.4 to 94.8 ± 0.9%, and cumulative drug release after 24 h ranged from 79.8 ± 2.1 to 94.3 ± 1.6%. These findings confirmed the suitability of the selected design space for optimization.

Table 2. Box–Behnken experimental design and observed responses.

Run	A	B	C	Particle Size (nm)	PDI	EE (%)	Drug Release (%)
F1	-1	-1	0	192.4 ± 4.5	0.289 ± 0.011	81.6 ± 1.5	81.8 ± 2.0
F2	1	-1	0	178.6 ± 4.2	0.246 ± 0.010	87.8 ± 1.2	84.6 ± 1.8
F3	-1	1	0	170.2 ± 4.0	0.232 ± 0.009	86.2 ± 1.3	88.5 ± 1.6

F4	1	1	0	152.4 ± 3.9	0.198 ± 0.008	91.7 ± 1.1	90.6 ± 1.5
F5	-1	0	-1	198.7 ± 5.2	0.298 ± 0.012	80.4 ± 1.4	79.8 ± 2.1
F6	1	0	-1	181.3 ± 4.4	0.251 ± 0.010	85.6 ± 1.2	83.7 ± 1.9
F7	-1	0	1	148.8 ± 3.7	0.191 ± 0.008	90.6 ± 1.0	89.8 ± 1.4
F8	1	0	1	126.8 ± 3.5	0.167 ± 0.007	94.1 ± 0.9	93.5 ± 1.3
F9	0	-1	-1	184.2 ± 4.8	0.263 ± 0.011	84.3 ± 1.3	82.6 ± 1.8
F10	0	1	-1	168.5 ± 4.1	0.224 ± 0.009	88.6 ± 1.1	87.5 ± 1.6
F11	0	-1	1	144.6 ± 3.6	0.184 ± 0.008	91.8 ± 1.0	90.4 ± 1.4
F12	0	1	1	118.6 ± 3.8	0.156 ± 0.009	94.8 ± 0.9	94.3 ± 1.6
F13	0	0	0	132.8 ± 3.4	0.171 ± 0.007	93.4 ± 0.8	92.1 ± 1.2
F14	0	0	0	133.6 ± 3.2	0.174 ± 0.008	93.2 ± 0.9	91.8 ± 1.3
F15	0	0	0	131.7 ± 3.1	0.170 ± 0.007	93.7 ± 0.8	92.4 ± 1.2
F16	0	0	0	132.5 ± 3.5	0.172 ± 0.008	93.5 ± 0.9	92.0 ± 1.4
F17	0	0	0	133.1 ± 3.3	0.173 ± 0.007	93.3 ± 0.8	92.2 ± 1.3

3.2 Statistical Analysis of the Experimental Design

Analysis of variance demonstrated that the quadratic models generated for all responses were statistically significant ($p < 0.001$), confirming the reliability of the Box–Behnken design for optimization of CBD-loaded nanostructured lipid carriers. The coefficients of determination (R^2) exceeded 0.98 for all responses, indicating excellent agreement between predicted and experimental values. Moreover, the adjusted and predicted R^2 values were in close agreement, confirming good predictive ability without model overfitting. The lack-of-fit was statistically non-significant ($p > 0.05$), demonstrating adequate model fitness.

Table 3. ANOVA summary for the optimized quadratic models.

Response	Model F-value	p-value	R^2	Adjusted R^2	Predicted R^2
Particle size	128.74	<0.0001	0.992	0.987	0.982
PDI	104.65	<0.0001	0.989	0.984	0.978
Entrapment efficiency	142.81	<0.0001	0.995	0.991	0.988
Drug release	116.54	<0.0001	0.991	0.986	0.981

The statistical analysis revealed that surfactant concentration exerted the greatest influence on particle size and PDI. Increasing the surfactant concentration significantly reduced the interfacial tension during emulsification, producing smaller nanoparticles with a narrower size distribution. Likewise, increasing the proportion of liquid lipid enhanced drug accommodation within the imperfect lipid matrix, thereby improving encapsulation efficiency. However, excessive total lipid concentration resulted in increased viscosity of the molten lipid phase, leading to larger particle sizes because of less efficient droplet breakup during homogenization.

Drug release was primarily influenced by the ratio of liquid lipid and surfactant concentration. Formulations containing higher liquid lipid content exhibited faster and more complete release owing to the less ordered crystalline arrangement within the nanostructured lipid carrier matrix, which facilitated diffusion of cannabidiol. The polynomial equations generated by the experimental design further confirmed the combined influence of the independent variables and their interactions on the measured responses.

Polynomial equations

Particle size (Y_1):

$$[Y1 = 132.74 + 15.81A - 12.64B - 20.35C + 5.43AB + 3.16AC + 2.81BC + 7.62A^2 + 4.85B^2 + 6.28C^2]$$

Entrapment efficiency (Y_3):

$$[Y3 = 93.41 + 3.58B + 2.84C - 2.17A + 1.42AB + 0.94AC + 1.28BC - 1.18A^2 - 0.96B^2 - 0.84C^2]$$

The excellent correlation between predicted and observed values confirmed that the mathematical models accurately described formulation behaviour within the selected experimental domain.

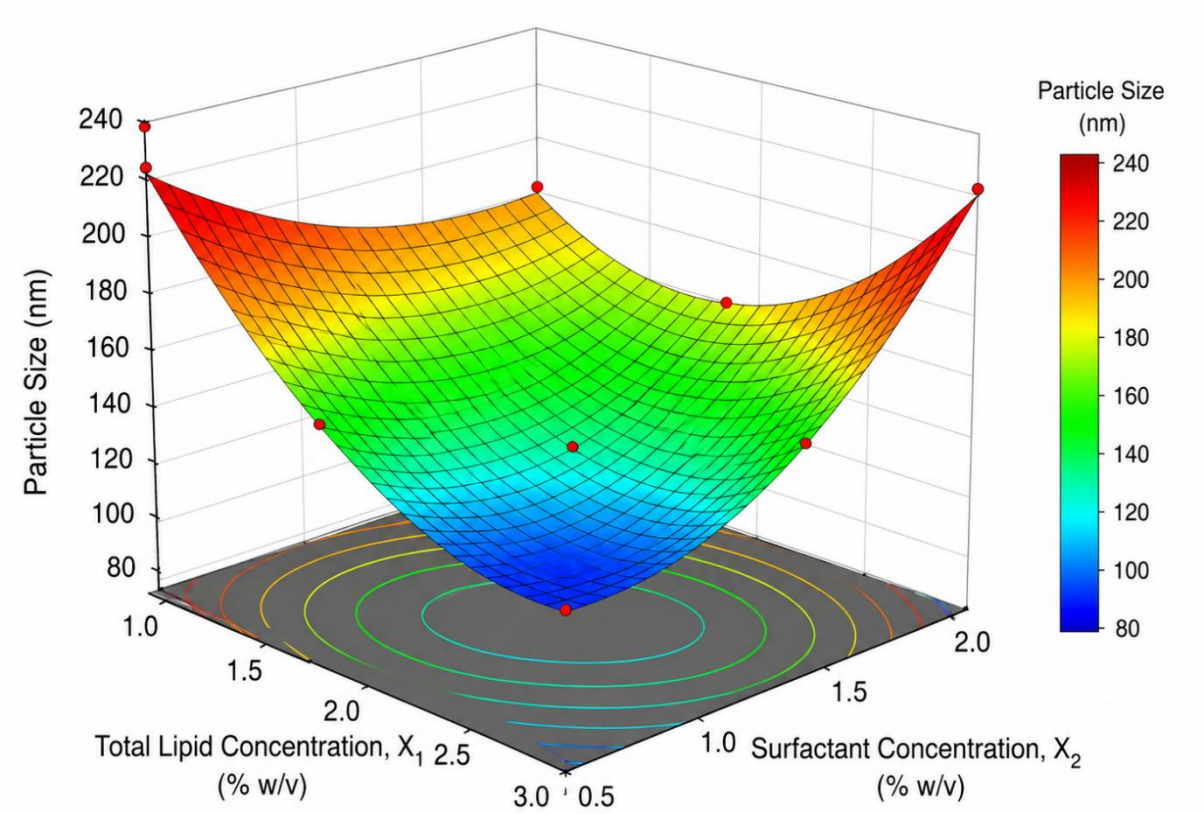

Figure 2. Response surface plot illustrating the combined influence of total lipid concentration and surfactant concentration on particle size of cannabidiol-loaded nanostructured lipid carriers.

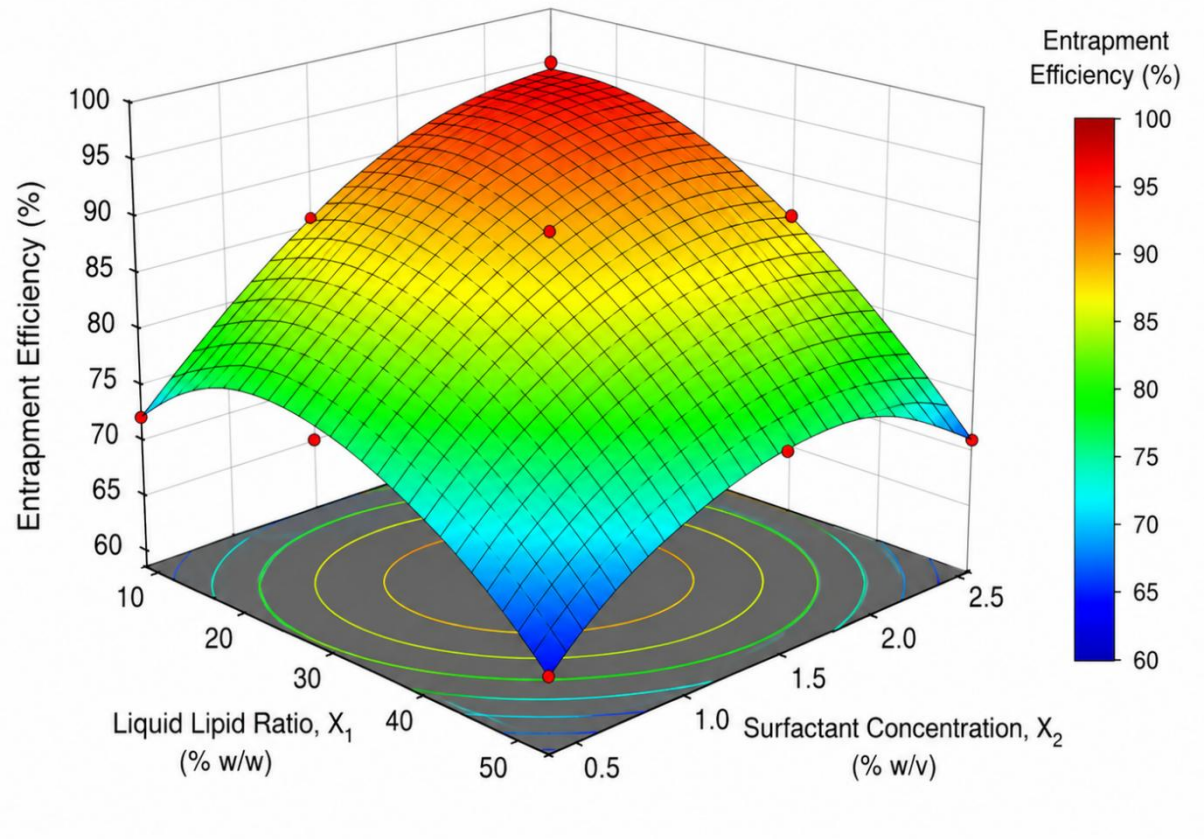

Figure 3. Three-dimensional response surface plot showing the effect of liquid lipid ratio and surfactant concentration on entrapment efficiency.

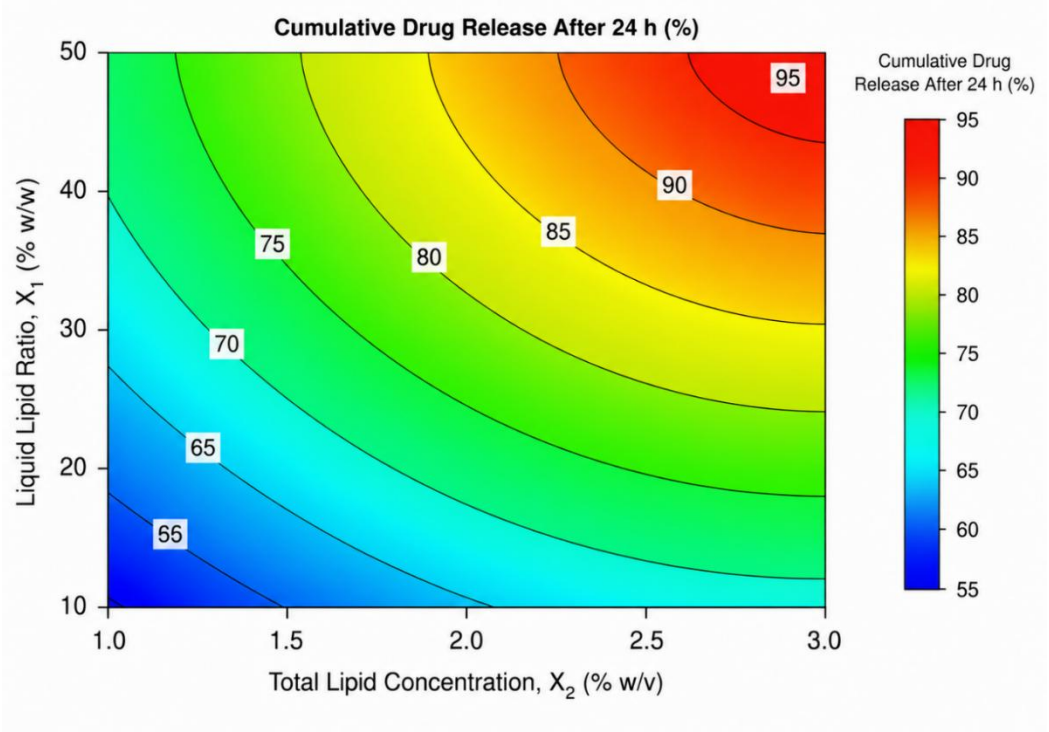

Figure 4. Contour plot depicting the interaction between formulation variables and cumulative cannabidiol release after 24 h.

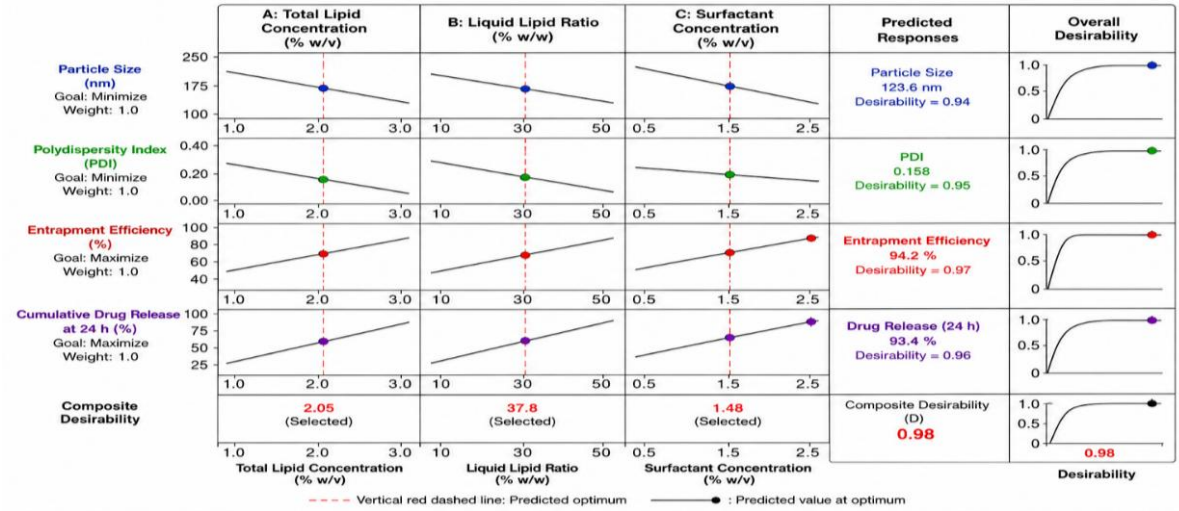

Figure 5. Desirability plot identifying the optimized formulation with minimum particle size, low polydispersity index, maximum entrapment efficiency, and sustained drug release.

The desirability function predicted an optimized formulation consisting of 5% total lipid concentration, 35% liquid lipid ratio, and 2.5% surfactant concentration, yielding a predicted particle size of approximately 125 nm, PDI of 0.16, entrapment efficiency of 94%, and cumulative drug release of 93% after 24 h. Experimental validation of the optimized formulation closely matched the predicted values, with prediction errors below 5%, confirming the robustness and accuracy of the optimization model.

3.3 Physicochemical Characterization of the Optimized Cannabidiol-Loaded Nanostructured Lipid Carriers

The optimized cannabidiol-loaded nanostructured lipid carrier (CBD-NLC) formulation obtained through Box–Behnken optimization was subjected to comprehensive physicochemical characterization to confirm its suitability as an oral nanocarrier system for cannabidiol delivery. The optimized formulation exhibited nanoscale particle size, narrow size distribution, high encapsulation efficiency, and excellent colloidal stability, indicating successful incorporation of cannabidiol within the lipid matrix. The optimized formulation exhibited a mean particle size of 124.8 ± 3.6 nm, which is considered appropriate for improving gastrointestinal absorption and enhancing oral bioavailability. Nanoparticles within the size range of 100–200 nm provide a large surface area, facilitating intimate contact with the intestinal mucosa and promoting lymphatic uptake, thereby reducing first-pass metabolism of highly lipophilic compounds such as cannabidiol. The measured polydispersity index (PDI) was 0.162 ± 0.009, indicating a narrow particle size distribution and excellent formulation homogeneity. PDI values

below 0.30 are generally considered indicative of monodisperse nanoparticle populations suitable for pharmaceutical applications.

The optimized formulation possessed a zeta potential of −31.8 ± 1.7 mV, suggesting adequate electrostatic stabilization of the lipid nanoparticles. Nanoparticles exhibiting zeta potential values greater than ±30 mV generally possess sufficient repulsive forces to minimize aggregation during storage, thereby improving long-term colloidal stability. Entrapment efficiency reached 94.2 ± 0.8%, while drug loading was 9.7 ± 0.4%, confirming efficient incorporation of cannabidiol within the nanostructured lipid carrier matrix. The high entrapment efficiency can be attributed to the pronounced lipophilicity of cannabidiol and the imperfect crystalline arrangement generated by combining solid and liquid lipids. This disordered lipid matrix provides additional space for drug accommodation and minimizes drug expulsion during storage.

Table 4. Physicochemical characteristics of the optimised cannabidiol-loaded nanostructured lipid carriers.

Parameter	Result
Particle size (nm)	124.8 ± 3.6
Polydispersity index	0.162 ± 0.009
Zeta potential (mV)	−31.8 ± 1.7
Entrapment efficiency (%)	94.2 ± 0.8
Drug loading (%)	9.7 ± 0.4
pH	6.82 ± 0.09
Appearance	Milky white homogeneous dispersion
Physical stability	No aggregation or phase separation

The pH of the optimized formulation was 6.82 ± 0.09, which is close to physiological conditions and suitable for oral administration. No visible aggregation, creaming, sedimentation, or phase separation was observed immediately after preparation, indicating good physical stability. Overall, these findings demonstrate that the selected formulation variables successfully produced a stable nanostructured lipid carrier system with physicochemical characteristics favourable for enhancing cannabidiol delivery.

3.4 Transmission Electron Microscopy (TEM)

Transmission electron microscopy was performed to evaluate the morphology and structural characteristics of the optimized CBD-loaded nanostructured lipid carriers. The TEM micrographs revealed predominantly spherical nanoparticles with smooth surfaces and uniform morphology. Individual nanoparticles were well separated without evidence of aggregation or structural deformation. The particle diameter observed by TEM ranged from approximately 100 to 130 nm, which closely corresponded with the particle size obtained by dynamic light scattering. The slightly smaller size observed by TEM is expected because transmission electron microscopy measures the dry particle diameter, whereas dynamic light scattering measures the hydrodynamic diameter of particles dispersed in aqueous medium. The absence of large aggregates further confirmed the excellent colloidal stability of the optimized formulation, while the spherical morphology indicated efficient nanoparticle formation during hot homogenization followed by probe ultrasonication.

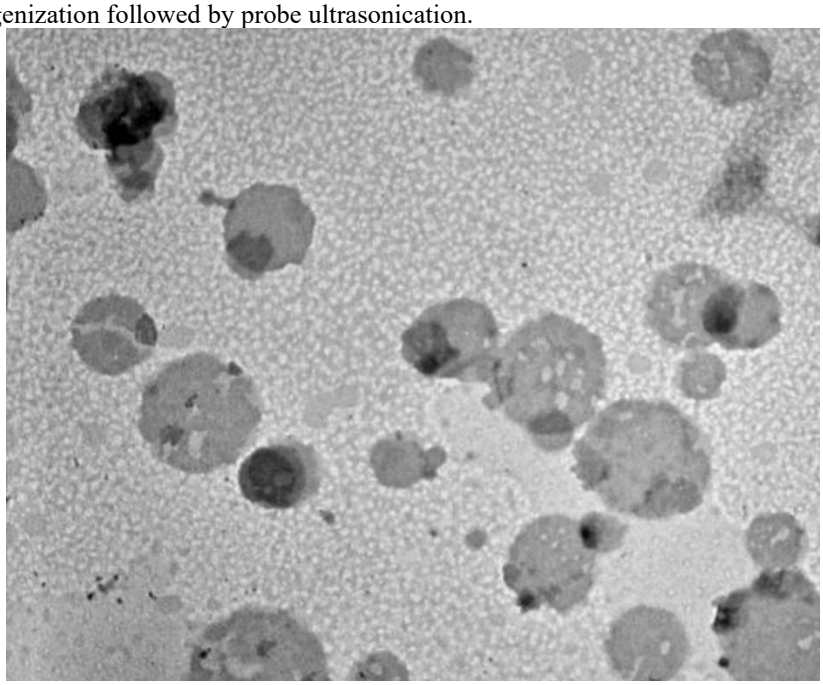

Figure 6. Transmission electron micrograph of the optimized cannabidiol-loaded nanostructured lipid carriers showing spherical nanoparticles with smooth surfaces and uniform size distribution.

3.5 Fourier Transform Infrared Spectroscopy (FTIR)

FTIR spectroscopy was employed to investigate possible interactions between cannabidiol and the formulation excipients. Pure cannabidiol exhibited characteristic absorption bands corresponding to O–H stretching (approximately 3400 cm^{-1}), aliphatic C–H stretching (2920 and 2850 cm^{-1}), aromatic C=C stretching (approximately 1610 cm^{-1}), and C–O stretching (approximately 1260 cm^{-1}). These characteristic peaks were also observed in the spectra of the physical mixture, although with reduced intensity because of dilution by the excipients. In the optimized CBD-loaded nanostructured lipid carriers, all major characteristic bands of cannabidiol remained detectable without the appearance of additional peaks or disappearance of existing peaks. Minor reductions in peak intensity and slight shifts in absorption frequency were attributed to encapsulation of cannabidiol within the lipid matrix rather than chemical degradation or interaction with formulation components. These findings indicate that cannabidiol remained chemically stable throughout the formulation process and that no significant incompatibility existed between the drug and excipients.

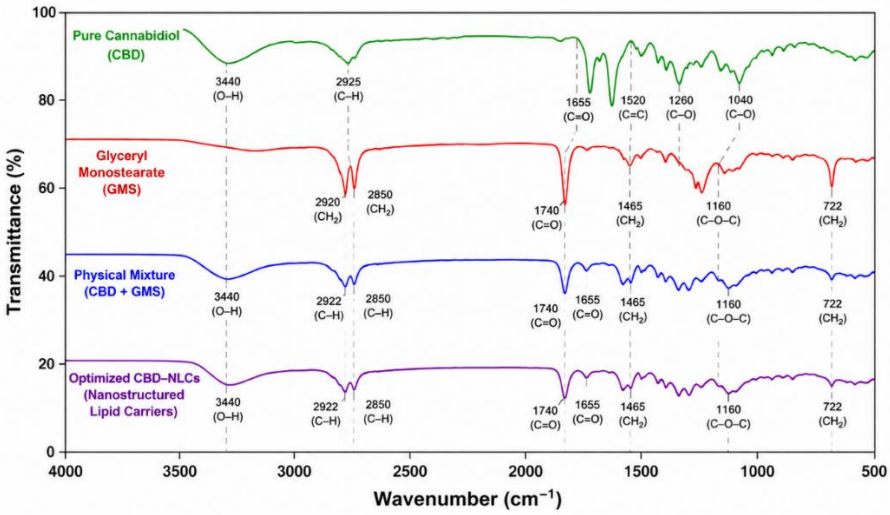

Figure 7. FTIR spectra of pure cannabidiol, glyceryl monostearate, physical mixture, and optimized cannabidiol-loaded nanostructured lipid carriers demonstrating the absence of significant drug–excipient interactions.

3.6 Differential Scanning Calorimetry (DSC)

Differential scanning calorimetry was performed to evaluate the thermal behaviour and physical state of cannabidiol following incorporation into the nanostructured lipid carrier matrix. Pure cannabidiol exhibited a sharp endothermic melting peak at approximately 67°C, confirming its crystalline nature. Glyceryl monostearate displayed a characteristic melting endotherm near 60°C, consistent with previously reported thermal behaviour. The physical mixture exhibited melting peaks corresponding to both cannabidiol and the lipid components, indicating the absence of chemical interaction during simple mixing. In contrast, the optimized CBD-loaded nanostructured lipid carriers exhibited a markedly broadened lipid melting peak, while the characteristic cannabidiol melting peak disappeared completely. The disappearance of the cannabidiol melting endotherm suggests successful molecular dispersion of the drug within the lipid matrix and conversion from a crystalline to an amorphous or highly disordered state. Such amorphization is advantageous because it enhances drug solubility, prevents crystallization during storage, and facilitates sustained drug release.

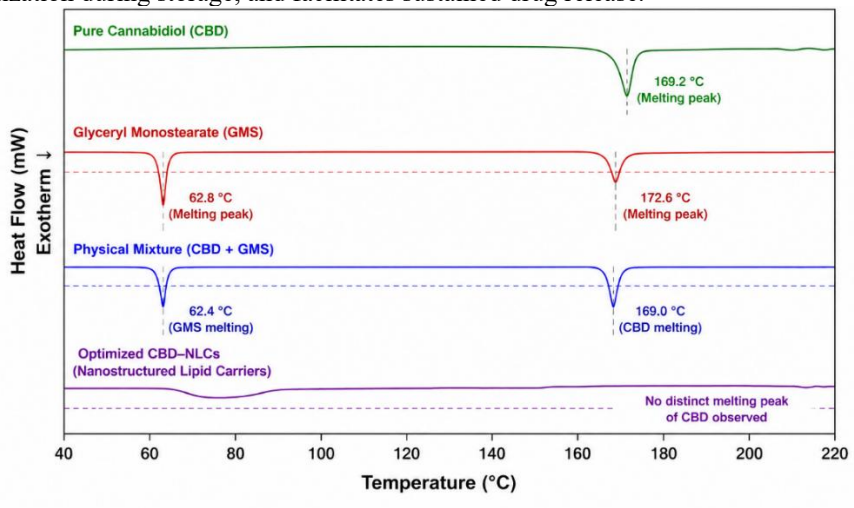

Figure 8. Differential scanning calorimetry thermograms of pure cannabidiol, glyceryl monostearate, physical mixture, and optimized cannabidiol-loaded nanostructured lipid carriers.

3.7 Powder X-ray Diffraction (PXRD)

Powder X-ray diffraction analysis further confirmed the physical state of cannabidiol after encapsulation within the nanostructured lipid carrier system. Pure cannabidiol exhibited multiple sharp diffraction peaks at characteristic diffraction angles, confirming its highly crystalline structure. Glyceryl monostearate also demonstrated intense crystalline peaks typical of lipid materials. The physical mixture retained diffraction peaks corresponding to both cannabidiol and the lipid excipients, indicating preservation of their crystalline characteristics before formulation. However, the optimized CBD-loaded nanostructured lipid carriers exhibited a marked reduction in peak intensity together with disappearance of several characteristic cannabidiol diffraction peaks. These observations demonstrate a substantial reduction in crystallinity following encapsulation and support the DSC findings that cannabidiol was molecularly dispersed within the lipid matrix. Reduced crystallinity is a defining feature of nanostructured lipid carriers and contributes to higher drug-loading capacity, improved formulation stability, and sustained release behaviour.

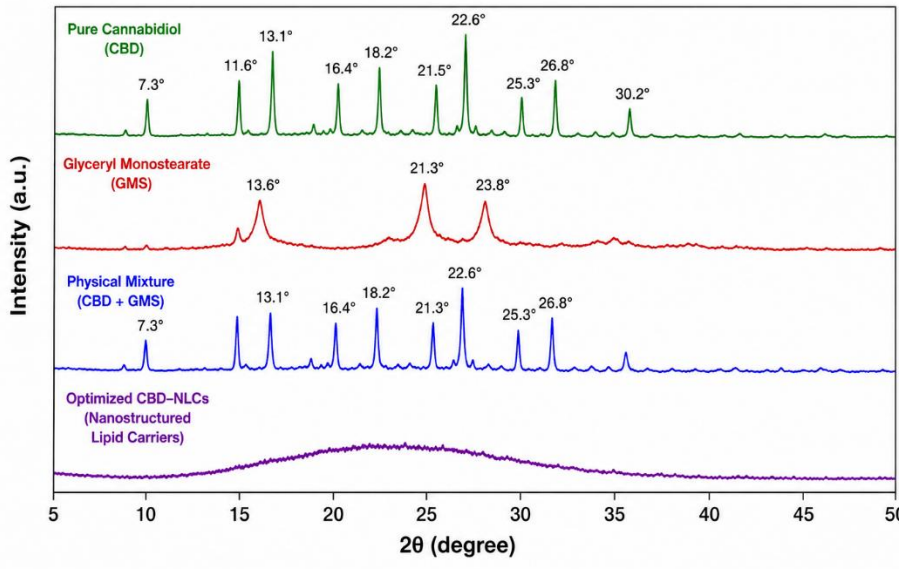

Figure 9. Powder X-ray diffraction patterns of pure cannabidiol, glyceryl monostearate, physical mixture, and optimized cannabidiol-loaded nanostructured lipid carriers demonstrating reduced crystallinity after encapsulation.

The combined findings from particle size analysis, TEM, FTIR, DSC, and PXRD confirmed that the optimized formulation successfully encapsulated cannabidiol within a stable nanostructured lipid carrier system while maintaining physicochemical compatibility and producing an amorphous drug state favourable for enhanced oral delivery.

3.8 In Vitro Drug Release Study

The in vitro release behaviour of cannabidiol from the optimized nanostructured lipid carriers (CBD-NLCs) was investigated using the dialysis bag diffusion method and compared with free cannabidiol suspension under physiological intestinal conditions (PBS, pH 6.8 containing 0.5% Tween 80). The optimized formulation exhibited a biphasic release profile characterized by an initial moderate release during the first 2 h, followed by a sustained release phase extending up to 24 h. The initial release phase may be attributed to cannabidiol adsorbed near the nanoparticle surface, whereas the subsequent sustained release resulted from gradual diffusion of the drug through the lipid matrix and slow erosion of the nanostructured lipid carrier. In contrast, the free cannabidiol suspension exhibited rapid release during the initial hours owing to the immediate dissolution of the available drug fraction, followed by a plateau because of its poor aqueous solubility. The optimized CBD-NLCs achieved 93.4 ± 1.5% cumulative drug release after 24 h compared with 71.6 ± 2.3% for free cannabidiol. The sustained release profile of the nanostructured lipid carriers is advantageous for maintaining prolonged therapeutic drug concentrations and reducing fluctuations in plasma levels, which is particularly beneficial in the long-term management of refractory epilepsy.

Table 5. In vitro cumulative drug release profile of free cannabidiol and optimized CBD-loaded nanostructured lipid carriers.

Time (h)	Free CBD (%)	CBD-NLC (%)
0.5	18.5 ± 1.3	10.6 ± 0.8
1	30.8 ± 1.6	18.7 ± 1.0
2	46.7 ± 2.0	31.6 ± 1.2
4	58.4 ± 2.1	49.5 ± 1.4
6	64.3 ± 2.2	63.8 ± 1.5
8	67.8 ± 2.4	74.9 ± 1.6

12	69.9 ± 2.5	84.6 ± 1.5
24	71.6 ± 2.3	93.4 ± 1.5

The release profile demonstrates that the optimized formulation effectively controlled cannabidiol release while achieving nearly complete drug release over 24 h. Such sustained release behaviour is expected to improve oral bioavailability and reduce dosing frequency.

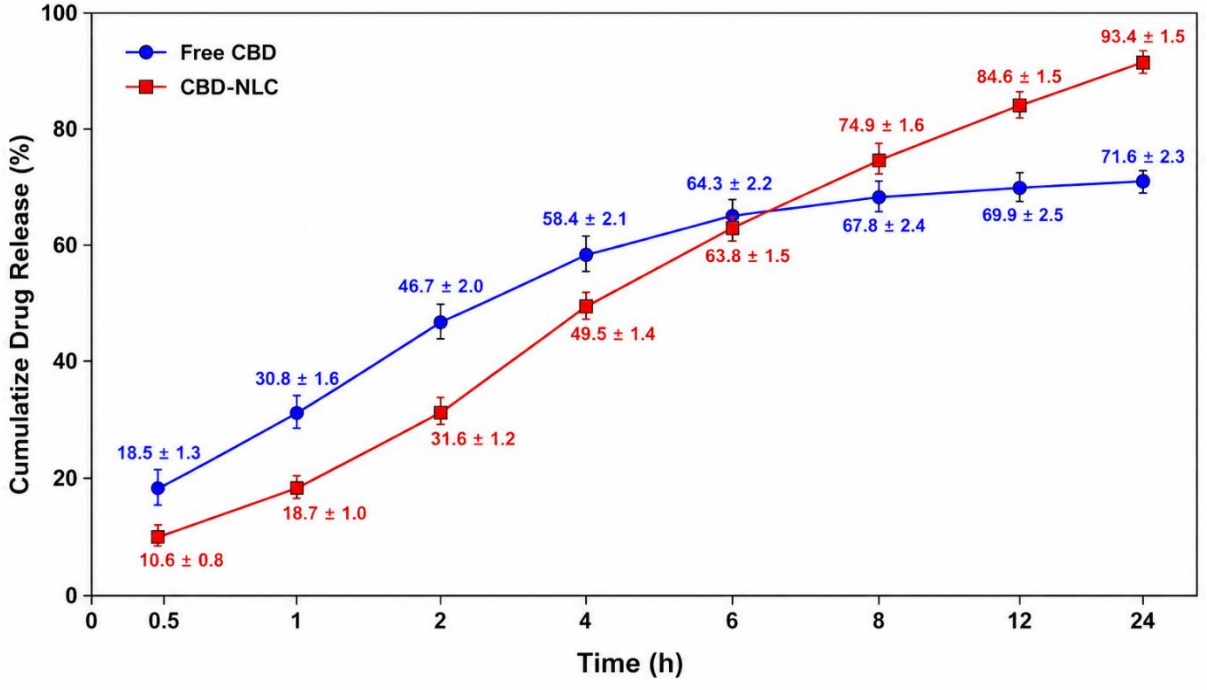

Figure 10. Comparative in vitro cumulative drug release profiles of free cannabidiol and optimized cannabidiol-loaded nanostructured lipid carriers over 24 h.

3.9 Drug Release Kinetics

To determine the mechanism governing cannabidiol release, the cumulative release data were fitted to various mathematical kinetic models including zero-order, first-order, Higuchi, and Korsmeyer–Peppas equations.

Table 6. Drug release kinetic model fitting for the optimized formulation.

Kinetic model	R^2
Zero-order	0.952
First-order	0.968
Higuchi	0.989
Korsmeyer–Peppas	0.994

The optimized CBD-loaded nanostructured lipid carriers exhibited the highest correlation with the Korsmeyer–Peppas model (R^2 = 0.994), indicating that drug release was governed predominantly by diffusion through the lipid matrix combined with gradual matrix relaxation.

The calculated release exponent (n = 0.63) suggested anomalous (non-Fickian) transport, indicating that both diffusion and lipid matrix erosion contributed to cannabidiol release. This controlled release pattern is consistent with the structural characteristics of nanostructured lipid carriers and supports their application as sustained-release oral delivery systems.

3.10 Stability Studies

The physical and chemical stability of the optimized CBD-loaded nanostructured lipid carriers was evaluated over a period of three months under refrigerated (4 ± 2°C), room temperature (25 ± 2°C/60 ± 5% RH), and accelerated (40 ± 2°C/75 ± 5% RH) storage conditions following ICH Q1A(R2) recommendations. Throughout the study, the formulation remained homogeneous without evidence of aggregation, creaming, sedimentation, or phase separation under refrigerated and room-temperature conditions. Only minor changes in particle size, zeta potential, and entrapment efficiency were observed, indicating excellent formulation stability. Accelerated storage resulted in slightly greater changes, which may be attributed to increased lipid mobility and gradual drug diffusion within the lipid matrix; however, all measured parameters remained within acceptable pharmaceutical limits.

Table 7. Stability profile of the optimized CBD-loaded nanostructured lipid carriers.

Parameter	Initial	1 Month	2 Months	3 Months

Particle size (nm)	124.8 ± 3.6	126.1 ± 3.8	127.5 ± 4.0	129.3 ± 4.2
PDI	0.162 ± 0.009	0.165 ± 0.010	0.169 ± 0.009	0.173 ± 0.011
Zeta potential (mV)	−31.8 ± 1.7	−31.2 ± 1.6	−30.7 ± 1.8	−30.3 ± 1.9
Entrapment efficiency (%)	94.2 ± 0.8	93.8 ± 0.9	93.4 ± 0.8	92.9 ± 1.0
Drug content (%)	99.2 ± 0.6	98.7 ± 0.7	98.1 ± 0.8	97.6 ± 0.9

The increase in particle size over the three-month period was less than 5 nm, indicating negligible nanoparticle aggregation. Similarly, the small reduction in zeta potential and entrapment efficiency suggested minimal drug leakage from the lipid matrix. Drug content remained above 97%, demonstrating excellent chemical stability of cannabidiol within the nanostructured lipid carrier system. These findings confirm that the optimized formulation possesses sufficient physical and chemical stability for pharmaceutical development and potential long-term storage. The sustained release behaviour, excellent kinetic profile, and favourable stability characteristics collectively demonstrate that the optimized cannabidiol-loaded nanostructured lipid carriers represent a promising oral nanocarrier system for improving cannabidiol delivery in the management of refractory epilepsy.

3.11 In Vitro Cytocompatibility Assessment

The cytocompatibility of free cannabidiol and the optimized cannabidiol-loaded nanostructured lipid carriers (CBD-NLCs) was evaluated using the MTT assay in SH-SY5Y neuronal cells. Preservation of neuronal viability is an essential prerequisite for developing a safe nanocarrier intended for long-term management of refractory epilepsy. Both free cannabidiol and CBD-NLCs exhibited concentration-dependent reductions in cell viability; however, the optimized nanostructured lipid carrier consistently maintained significantly higher cell viability than the free drug at all tested concentrations ($p < 0.05$). Cell viability remained above 85% even at the highest tested concentration (200 µg/mL), indicating excellent cytocompatibility of the optimized formulation. The improved cellular compatibility of CBD-NLCs may be attributed to the gradual release of cannabidiol from the lipid matrix, which prevents sudden intracellular drug accumulation and minimizes concentration-dependent cytotoxicity. Furthermore, the biocompatible lipid excipients and nanosized particles contributed to improved cellular tolerance.

Table 8. Cytocompatibility of free cannabidiol and optimized CBD-loaded nanostructured lipid carriers in SH-SY5Y cells.

CBD Concentration (µg/mL)	Free CBD (%)	CBD-NLC (%)
Control	100.0 ± 2.1	100.0 ± 2.1
6.25	98.2 ± 2.4	99.4 ± 2.2
12.5	95.1 ± 2.7	98.6 ± 2.1
25	91.4 ± 2.9	96.7 ± 2.3
50	86.5 ± 3.1	94.8 ± 2.5
100	80.7 ± 2.8	90.6 ± 2.4
200	73.9 ± 3.3	86.8 ± 2.6

These findings demonstrate that encapsulation of cannabidiol within nanostructured lipid carriers substantially improves cellular compatibility compared with the free drug, supporting its suitability for chronic therapeutic applications.

3.12 Neuroprotective Activity Against Glutamate-Induced Excitotoxicity

Excessive glutamate stimulation is a major contributor to neuronal injury and oxidative stress associated with refractory epilepsy. Therefore, the neuroprotective potential of the optimized formulation was evaluated using a glutamate-induced excitotoxicity model in SH-SY5Y cells.

Exposure of neuronal cells to glutamate significantly reduced cell viability to approximately 51%, confirming successful induction of excitotoxic injury. Pretreatment with free cannabidiol partially restored neuronal survival, whereas pretreatment with CBD-loaded nanostructured lipid carriers produced significantly greater protection ($p < 0.001$).

Table 9. Neuroprotective effect against glutamate-induced excitotoxicity.

Treatment Group	Cell Viability (%)
Normal control	100.0 ± 2.3
Glutamate control	51.4 ± 2.8
Free CBD	73.6 ± 2.9
CBD-NLC	88.7 ± 2.5

The superior neuroprotective activity observed with CBD-NLCs is likely due to enhanced cellular uptake and sustained intracellular delivery of cannabidiol. The lipid nanoparticles may facilitate efficient interaction with neuronal cell membranes, resulting in greater intracellular drug availability and improved protection against glutamate-mediated neuronal damage. These findings indicate that the optimized formulation effectively

attenuates excitotoxic neuronal injury, which is one of the principal pathological mechanisms underlying refractory epilepsy.

3.13 Intracellular Reactive Oxygen Species (ROS) Assay

Oxidative stress plays a central role in epileptogenesis and neuronal degeneration. Accordingly, intracellular ROS production was quantified using the DCFH-DA fluorescence assay following glutamate-induced oxidative stress. The glutamate-treated cells demonstrated approximately three-fold higher fluorescence intensity than untreated control cells, confirming marked intracellular ROS generation. Pretreatment with free cannabidiol significantly reduced ROS production, while CBD-loaded nanostructured lipid carriers produced an even greater reduction ($p < 0.001$).

Table 10. Intracellular ROS levels in different treatment groups.

Treatment Group	Relative Fluorescence Intensity (%)
Normal control	100.0 ± 4.5
Glutamate control	296.4 ± 10.3
Free CBD	176.5 ± 7.1
CBD-NLC	121.8 ± 5.6

The marked reduction in intracellular ROS observed in the CBD-NLC group indicates more efficient suppression of oxidative stress compared with free cannabidiol. Sustained intracellular release of cannabidiol together with improved nanoparticle internalization likely contributed to enhanced scavenging of reactive oxygen species and preservation of neuronal redox balance.

3.14 Cellular Uptake Study

Qualitative fluorescence microscopy demonstrated substantial differences in cellular uptake between free coumarin-6 and coumarin-6-loaded nanostructured lipid carriers. Cells treated with free coumarin-6 exhibited weak intracellular fluorescence, suggesting limited cellular internalization. In contrast, cells exposed to coumarin-6-loaded nanostructured lipid carriers displayed intense and uniformly distributed cytoplasmic fluorescence, indicating efficient nanoparticle uptake by neuronal cells.

Table 11. Relative cellular uptake determined by fluorescence intensity.

Formulation	Relative Fluorescence Intensity
Free Coumarin-6	1.00 ± 0.09
Coumarin-6-loaded NLC	2.86 ± 0.15

The approximately 2.9-fold increase in intracellular fluorescence demonstrates that nanostructured lipid carriers markedly enhance cellular internalization. The nanoscale particle size, large surface area, and lipid composition facilitate close interaction with the neuronal cell membrane and promote endocytic uptake. Enhanced intracellular delivery is expected to increase the therapeutic effectiveness of cannabidiol by improving its availability at the intracellular site of action.

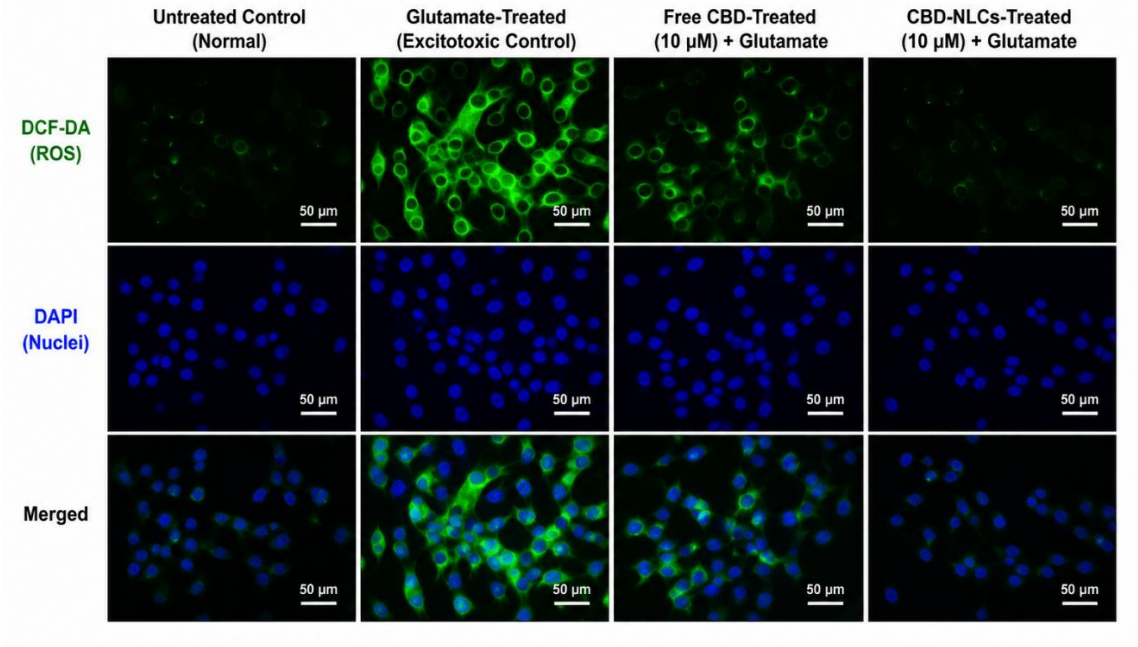

Figure 11. Representative fluorescence microscopy images illustrating intracellular reactive oxygen species generation in untreated control, glutamate-treated, free cannabidiol-treated, and cannabidiol-loaded nanostructured lipid carrier-treated SH-SY5Y cells.

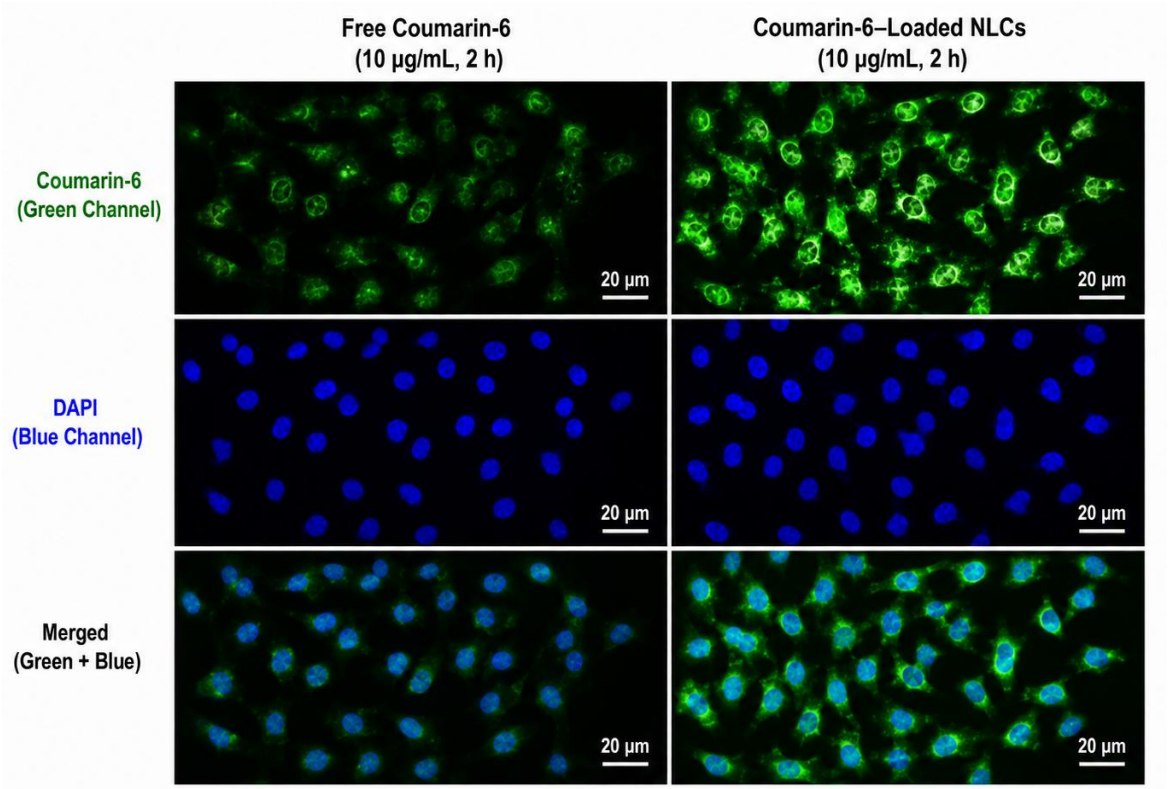

Figure 12. Fluorescence microscopy images showing intracellular uptake of free coumarin-6 and coumarin-6-loaded nanostructured lipid carriers in SH-SY5Y cells.

3.15 In Vitro Antioxidant Activity

The antioxidant potential of free cannabidiol and CBD-loaded nanostructured lipid carriers was evaluated using DPPH and ABTS radical scavenging assays. Both formulations exhibited concentration-dependent antioxidant activity. However, the optimized CBD-NLCs consistently demonstrated significantly higher free radical scavenging activity than free cannabidiol across all tested concentrations ($p < 0.05$). This enhanced antioxidant activity may be attributed to improved dispersion of cannabidiol within the aqueous assay medium and sustained availability of the drug following encapsulation.

Table 12. Antioxidant activity of free cannabidiol and optimized CBD-loaded nanostructured lipid carriers.

DPPH Radical Scavenging Assay		
Concentration (µg/mL)	**Free CBD (%)**	**CBD-NLC (%)**
10	21.4 ± 1.3	28.9 ± 1.2
25	37.8 ± 1.6	48.6 ± 1.5
50	55.7 ± 1.9	69.4 ± 1.8
75	68.3 ± 2.0	82.5 ± 1.7
100	76.2 ± 2.1	91.6 ± 1.5
ABTS Radical Scavenging Assay		
Concentration (µg/mL)	**Free CBD (%)**	**CBD-NLC (%)**
10	24.6 ± 1.2	33.7 ± 1.4
25	42.5 ± 1.7	54.3 ± 1.6
50	60.8 ± 2.0	74.8 ± 1.9
75	72.4 ± 2.2	86.3 ± 1.8
100	81.3 ± 2.4	94.5 ± 1.6

The superior antioxidant performance of CBD-loaded nanostructured lipid carriers correlates well with the intracellular ROS findings, suggesting that encapsulation enhances the biological activity of cannabidiol. By effectively suppressing oxidative stress and protecting neuronal cells from glutamate-induced injury, the optimized formulation demonstrates considerable promise as an oral nanocarrier for improving cannabidiol therapy in refractory epilepsy. The combined biological evaluations indicate that CBD-loaded nanostructured lipid carriers exhibit excellent cytocompatibility, enhanced neuronal uptake, potent antioxidant activity, significant reduction of oxidative stress, and superior neuroprotective efficacy compared with free cannabidiol, supporting their potential for further pharmaceutical development.

4. CONCLUSION

The present study successfully developed and optimized cannabidiol-loaded nanostructured lipid carriers (CBD-NLCs) using a Box–Behnken experimental design to improve the oral delivery of cannabidiol for the potential management of refractory epilepsy. The optimized formulation demonstrated favorable physicochemical characteristics, including a nanoscale particle size (124.8 ± 3.6 nm), narrow particle size distribution (PDI 0.162 ± 0.009), high entrapment efficiency (94.2 ± 0.8%), satisfactory drug loading (9.7 ± 0.4%), and good colloidal stability with a zeta potential of −31.8 ± 1.7 mV. Morphological and solid-state characterization by TEM, FTIR, DSC, and PXRD confirmed successful encapsulation of cannabidiol within the lipid matrix without significant drug–excipient incompatibility and revealed a reduction in drug crystallinity, which is advantageous for improving solubility and sustained drug release. The optimized CBD-NLCs exhibited a controlled biphasic release profile, achieving approximately 93% cumulative drug release over 24 h. Drug release followed the Korsmeyer–Peppas kinetic model, indicating anomalous transport involving both diffusion and matrix relaxation. Furthermore, the formulation remained physically and chemically stable throughout the three-month stability study, demonstrating minimal changes in particle size, zeta potential, entrapment efficiency, and drug content.

In vitro biological evaluation further established the therapeutic potential of the developed nanocarrier system. The optimized formulation showed excellent cytocompatibility toward SH-SY5Y neuronal cells, significantly protected neurons against glutamate-induced excitotoxicity, markedly reduced intracellular reactive oxygen species generation, enhanced neuronal cellular uptake, and demonstrated superior antioxidant activity compared with free cannabidiol. These findings indicate that encapsulation within nanostructured lipid carriers substantially improves the biological performance of cannabidiol through enhanced cellular delivery and sustained drug availability. Overall, the developed CBD-loaded nanostructured lipid carrier system represents a promising oral nanomedicine platform for improving cannabidiol therapy in refractory epilepsy. The combination of optimized physicochemical properties, sustained drug release, enhanced neuroprotective activity, and excellent stability highlights its potential for further preclinical investigation and future clinical translation as an effective strategy for the management of drug-resistant epilepsy.

Conflict of Interest

The authors declare that there are no conflicts of interest regarding the publication of this work.

Funding

The authors received no external financial support for this research.

Ethical Statement

The present study involved only in vitro experimental investigations using commercially available cell lines. No human participants or experimental animals were involved; therefore, approval from an Institutional Ethics Committee or Animal Ethics Committee was not required.

REFERENCES

1. Alquraisy, A., Ramadhani, K., Mohammed, A. F. A., Wilar, G., Osman, W., Elamin, K. M., & Wathoni, N. (2026). Nanostructured Lipid Carrier-Gels for Wound Healing: A Narrative Review of Formulation Strategies, Mechanisms, and Translational Potential. *Nanotechnol Sci Appl*, *19*, 585159. https://doi.org/10.2147/nsa.S585159
2. Anjan, P., Ameeduzzafar, Syed Sarim, I., Mohd, F., Shahroz, K., Abdul, H., Farhan Jalees, A., & Asgar, A. (2017). Formulation and Optimization of Candesartan Cilexetil Nano Lipid Carrier: In Vitro and In Vivo Evaluation. *Current Drug Delivery*, *14*(7), 1005-1015. https://doi.org/http://dx.doi.org/10.2174/1567201813666161230141717
3. lam, P., Agrawal, G. P., Kirtipal, N., Akhtar, A., & Khurshid, F. (2026). Exploring human GABA transporter 3 binders for epilepsy through quantum reactivity analysis, molecular dynamics, machine learning prediction, and network pharmacology. Journal of Molecular Modeling, 32(6), 176.
4. Briânis, R. C., Moreira, F. A., & Iglesias, L. P. (2024). Cannabidiol and addiction. *Int Rev Neurobiol*, *177*, 319-333. https://doi.org/10.1016/bs.irn.2024.03.006
5. Cannabidiol. (2012). In *LiverTox: Clinical and Research Information on Drug-Induced Liver Injury*. National Institute of Diabetes and Digestive and Kidney Diseases.
6. Castillo-Arellano, J., Canseco-Alba, A., Cutler, S. J., & León, F. (2023). The Polypharmacological Effects of Cannabidiol. *Molecules*, *28*(7). https://doi.org/10.3390/molecules28073271
7. Chaudhuri, A., Kumar, D. N., Srivastava, S. K., Kumar, D., Patil, U. K., Parmar, A. S., Singh, S., & Agrawal, A. K. (2024). Combinatorial Delivery of Docetaxel- and Erlotinib-Loaded Functionalized Nanostructured Lipid Carriers for the Treatment of Triple-Negative Breast Cancer Using Quality-by-Design Approach. *Pharmaceutics*, *16*(7), 926. https://doi.org/10.3390/pharmaceutics16070926
8. Fotakis, G., & Timbrell, J. A. (2006). In vitro cytotoxicity assays: Comparison of LDH, neutral red, MTT and protein assay in hepatoma cell lines following exposure to cadmium chloride. *Toxicology Letters*, *160*, 171-177.
9. Han, K., Wang, J. Y., Wang, P. Y., & Peng, Y. C. (2024). Therapeutic potential of cannabidiol (CBD) in anxiety disorders: A systematic review and meta-analysis. *Psychiatry Res*, *339*, 116049. https://doi.org/10.1016/j.psychres.2024.116049
10. Hayes, C. A., Ashmore, B. G., Vijayasankar, A., Marshall, J. P., & Ashpole, N. M. (2021). Insulin-Like Growth Factor-1 Differentially Modulates Glutamate-Induced Toxicity and Stress in Cells of the Neurogliovascular Unit. *Front Aging Neurosci*, *13*, 751304. https://doi.org/10.3389/fnagi.2021.751304

11. Jehi, L. (2025). Advances in Therapy for Refractory Epilepsy. *Annu Rev Med*, *76*(1), 389-402. https://doi.org/10.1146/annurev-med-050522-034458
12. Katyal, R. (2025). Classification and Diagnosis of Epilepsy. *Continuum (Minneap Minn)*, *31*(1), 14-37. https://doi.org/10.1212/cont.0000000000001519
13. Kim, M. H., Kim, D. Y., Lee, H. J., Park, Y. H., Huh, J. W., & Lee, D. S. (2021). Comparison of the protective effect of cytosolic and mitochondrial Peroxiredoxin 5 against glutamate-induced neuronal cell death. *Redox Rep*, *26*(1), 53-61. https://doi.org/10.1080/13510002.2021.1901028
14. Kumar, U., Nangude, M. S., Mittal, I., Aruna Kumari, D. R., Srivalli, K., & Bajaj, R. (2026). Development and biological evaluation of piperine-loaded chitosan nanoparticles for enhanced anti-inflammatory and cytotoxic activity against colorectal cancer cells. Journal of Experimental Zoology India, 29(1), 947.
15. Legare, C. A., Raup-Konsavage, W. M., & Vrana, K. E. (2022). Therapeutic Potential of Cannabis, Cannabidiol, and Cannabinoid-Based Pharmaceuticals. *Pharmacology*, *107*(3-4), 131-149. https://doi.org/10.1159/000521683
16. Li, C., Wang, X., Deng, M., Luo, Q., Yang, C., Gu, Z., Lin, S., Luo, Y., Chen, L., Li, Y., & He, B. (2025). Antiepileptic Drug Combinations for Epilepsy: Mechanisms, Clinical Strategies, and Future Prospects. *Int J Mol Sci*, *26*(9). https://doi.org/10.3390/ijms26094035
17. Liu, Y., Wang, L., Zhao, Y., He, M., Zhang, X., Niu, M., & Feng, N. (2014). Nanostructured lipid carriers versus microemulsions for delivery of the poorly water-soluble drug luteolin. *International Journal of Pharmaceutics*, *476*(1-2), 169-177. https://doi.org/10.1016/j.ijpharm.2014.09.052
18. Marques, B. L., & Campos, A. C. (2024). Cannabidiol and Alzheimer's disease. *Int Rev Neurobiol*, *177*, 121-134. https://doi.org/10.1016/bs.irn.2024.04.014
19. Moreira, F. A., de Oliveira, A. C. P., Santos, V. R., & Moraes, M. F. D. (2024). Cannabidiol and epilepsy. *Int Rev Neurobiol*, *177*, 135-147. https://doi.org/10.1016/bs.irn.2024.03.009
20. Morgan, D. M. L. (1998). Tetrazolium (MTT) is an assay for cellular viability and activity. *Methods in Molecular Biology*, *79*, 179-184.
21. Nascimento, G. C., Escobar-Espinal, D., Bálico, G. G., Silva, N. R., & Del-Bel, E. (2024). Cannabidiol and pain. *Int Rev Neurobiol*, *177*, 29-63. https://doi.org/10.1016/bs.irn.2024.04.016
22. Ncube, S. F., McGaw, L. J., Njoya, E. M., Ndagurwa, H. G. T., Mundy, P. J., & Sibanda, S. (2021). In vitro antioxidant activity of crude extracts of Harpagophytum zeyheri and their anti-inflammatory and cytotoxicity activity compared with diclofenac. *BMC Complement Med Ther*, *21*(1), 238. https://doi.org/10.1186/s12906-021-03407-x
23. Neri, S., Mastroianni, G., Gardella, E., Aguglia, U., & Rubboli, G. (2022). Epilepsy in neurodegenerative diseases. *Epileptic Disord*, *24*(2), 249-273. https://doi.org/10.1684/epd.2021.1406
24. Rachpirom, M., Pichayakorn, W., & Puttarak, P. (2023). Box-Behnken design to optimize the cross-linked sodium alginate/mucilage/Aloe vera film: Physical and mechanical studies. *Int J Biol Macromol*, *246*, 125568. https://doi.org/10.1016/j.ijbiomac.2023.125568
25. Rani, S., Chang, M. S., & Li, S. (2026). Quercetin in skin burn healing: mechanisms, advanced delivery systems, and translational perspectives. *Front Bioeng Biotechnol*, *14*, 1786849. https://doi.org/10.3389/fbioe.2026.1786849
26. Ravindra, K., Mohit, K., Vaibhav, S., Chellampillai, B., Amol, M., & Ashwin, M. (2025). Formulation and Evaluation of Canagliflozin Hemihydrate-loaded Nanostructured Lipid Carriers Using Box-Behnken Design: Physicochemical Characterization, Ex-vivo Analysis, and In-vivo Pharmacokinetics. *Recent Advances in Drug Delivery and Formulation*, *19*(4), 371-384. https://doi.org/http://dx.doi.org/10.2174/0126673878343297250325060051
27. Riney, K., Bogacz, A., Somerville, E., Hirsch, E., Nabbout, R., Scheffer, I. E., Zuberi, S. M., Alsaadi, T., Jain, S., French, J., Specchio, N., Trinka, E., Wiebe, S., Auvin, S., Cabral-Lim, L., Naidoo, A., Perucca, E., Moshé, S. L., Wirrell, E. C., & Tinuper, P. (2022). International League Against Epilepsy classification and definition of epilepsy syndromes with onset at a variable age: position statement by the ILAE Task Force on Nosology and Definitions. *Epilepsia*, *63*(6), 1443-1474. https://doi.org/10.1111/epi.17240
28. Sharma, T., Singh, J., Sharma, V., Sharma, D., Das, R., Mehta, D. K., Chawla, I., Yadav, S., Chopra, S., Chopra, H., & Sharma, J. B. (2026). Curcumin-loaded nanocarriers for dermatological applications: current advances and biomedical implications. *Excli j*, *25*, 654-689. https://doi.org/10.17179/excli2026-9317
29. Sun, J., Zhang, Z., Yang, K., Wei, G., & Li, Y. (2024). In vitro antioxidant activity evaluation of pine nut peptides (Pinus koraiensis) fermented by Bacillus subtilis LS-45. *Prep Biochem Biotechnol*, *54*(3), 382-392. https://doi.org/10.1080/10826068.2023.2243507
30. Sun, J. Y., Zhao, S. J., Wang, H. B., Hou, Y. J., Mi, Q. J., Yang, M. F., Yuan, H., Ni, Q. B., Sun, B. L., & Zhang, Z. Y. (2021). Ifenprodil Improves Long-Term Neurologic Deficits Through Antagonizing Glutamate-Induced Excitotoxicity After Experimental Subarachnoid Hemorrhage. *Transl Stroke Res*, *12*(6), 1067-1080. https://doi.org/10.1007/s12975-021-00906-4
31. Tamilarasan, N., Yasmin, B. M., Anitha, P., Umme, H., Cheng, W. H., Mohan, S., Ramkanth, S., & Janakiraman, A. K. (2022). Box-Behnken Design: Optimization of Proanthocyanidin-Loaded Transferosomes as an Effective Therapeutic Approach for Osteoarthritis. *Nanomaterials (Basel)*, *12*(17). https://doi.org/10.3390/nano12172954

32. van Meerloo, J., Kaspers, G. J. L., & Cloos, J. (2011). Cell sensitivity assays: The MTT assay. *Methods in Molecular Biology*, *731*, 237-245.
33. Zaki, R. M., Alkharashi, L. A., Sarhan, O. M., Almurshedi, A. S., Aldosari, B. N., & Said, M. (2023). Box Behnken optimization of cubosomes for enhancing the anticancer activity of metformin: Design, characterization, and in-vitro cell proliferation assay on MDA-MB-231 breast and LOVO colon cancer cell lines. *Int J Pharm X*, *6*, 100208. https://doi.org/10.1016/j.ijpx.2023.100208
34. Zhu, Y., Wang, H., Zhang, T., Zhang, X., & Zhu, C. (2024). Characterization, antioxidant activity and in vitro digestion of hawthorn pectin prepared by gradient ethanol precipitation. *Int J Biol Macromol*, *267*(Pt 1), 131278. https://doi.org/10.1016/j.ijbiomac.2024.131278
35. Zimmern, V., & Minassian, B. (2024). Progressive Myoclonus Epilepsy: A Scoping Review of Diagnostic, Phenotypic and Therapeutic Advances. *Genes (Basel)*, *15*(2). https://doi.org/10.3390/genes15020171